A Time and Energy Efficient Multi-UAV Coverage Planning for the Search and Rescue Mission under Wind fields

ING-CHAU CHANG, MEN-YI LI, YU-HSUAN HSIEH, CHIN-EN YEN
Department of Computer Science and Information Engineering,
National Changhua University of Education, Chaunghua County, TAIWAN

Abstract: — This paper discusses how to quickly and efficiently search for victims when a disaster occurs. Since the search area is large, the search time of a single UAV will be too long to satisfy the golden window of the search and rescue mission. Therefore, it is necessary to dispatch multiple UAVs to conduct a cooperative search by proposing a multi-UAV area coverage planning under wind fields (MUCPW) algorithm and its variant MUCPW-A to achieve the shortest mission time. It first averagely divides the search area into several regions, formulates equations to calculate the minimum mission time and corresponding energy consumption among all possible area partition methods. As compared to related work, simulation results show that MUCPW and MUCPW-A achieve the shortest mission time and the least energy consumption to search all victims in the search and rescue mission. Further, MUCPW-A achieves the smallest standard deviation in energy consumption.

Key-words: —unmanned aerial vehicles, wind fields, disaster events, coverage planning, multi-UAV cooperation.

Received: March 12, 2024. Revised: August 2, 2024. Accepted: September 11, 2024. Published: October 9, 2024.

1.Introduction

Unmanned Aerial Vehicles (UAVs), distinguished by their superior features compared to ground vehicles, including high maneuverability, the capability to navigate obstacles during motion, independence from terrain constraints, and the installation of cameras for improved visibility, have garnered widespread favor across various domains [1]. Particularly in the realm of search and rescue (SAR) operations, UAVs are dispatched to systematically investigate and gather crucial search intelligence. They serve as effective substitutes for human exploration in disaster-stricken areas characterized by rugged terrain and hazardous environments. Beyond enhancing operational efficiency, this utilization of UAVs also significantly reduces potential risks for rescue personnel.

In research [2], UAVs are mentioned to employ Boustrophedon (derived from the Greek word meaning "ox path") path planning when traversing convex polygonal regions by back-and-forth searches in the area. The real-time wind speed and direction significantly affects the search time and energy consumption of the UAV. The starting and ending units of the SAR mission, the choice between horizontal and vertical UAV flight directions and the corresponding length of the UAV flight path are depending on the wind fields. Priority is given to search the region of the mission area that is farthest from the Ground Control Station (GCS), mitigating potential issues such as insufficient battery power or overlapping routes when the UAV completes its search and returns to the GCS.

This research makes the following contributions. Aiming to achieve the shortest search time and consumed power of the SAR mission, we propose a Multi-UAV Coverage Planning under Wind fields (MUCPW) algorithm and its search process. The approach involves initially dividing the entire SAR mission area into multiple regions. Depending on the real-time UAV hover altitude and flight speed and the wind direction and speed, the GCS utilizes the MUCPW algorithm to calculate the optimal region partitioning choice by computing the starting and ending units as well as the search path length and corresponding energy consumption for each region. Equations for calculating the SAR mission time and energy consumption are formulated. Simulation experiments are conducted by varying the area size and the number of UAVs to compare the search time and the UAV energy consumption between the proposed MUCPW and two related studies, LSAR and LIAM.

2.Literature Review

Research [3] discussed the balanced path planning of multiple UAVs for various dispersed regions. In the study, the starting UAV position for each dispersed region is assumed to be known. Each UAV departs from the same GCS to traverse multiple dispersed regions and the mission is considered complete after visiting the last region, without the need for UAVs to return to the GCS. During the exploration of each region, UAVs follow the shortest path, i.e., a straight-line flight, to reach the next area. A notable drawback lacks consideration for wind fields and UAV collaboration issues throughout the entire process. In research [4], the system was divided into two main components: region partition and path planning. The study focuses on effective partitioning of large regular polygons to facilitate disaster inspections and soil degradation monitoring. Multiple UAVs are employed in a flight planning system. The authors have devised an efficient method for region partitioning, considering UAV flight time constraints and collision avoidance through the effective path planning. However, a drawback lacks consideration for environmental factors and UAV fly duration in the approach.

In research [5], multiple UAVs were deployed for SAR missions, with tasks assigned based on the remaining battery capacity of each UAV. The search area was divided into blocks of size $3a \times 3a$, depending on the number of UAVs. The area is equally distributed among all UAVs. Each UAV conducts a slow and random search within its assigned area until the exploration is completed or the battery level reaches a predefined threshold. This work lacks consideration for the impact of wind fields. Its search methodology relies on a random approach, potentially resulting in UAV energy wastage on duplicated paths. In research [6], the use of multiple UAVs was discussed for disaster response. The paper

introduced the layered SAR approach, acknowledging that the number of casualties decreases gradually as the disaster center expands outward. The proposed method divides the disaster area into several layers, with decreasing weights assigned from the center outward. However, it lacks consideration for environmental factors and the issue of UAV battery capacity.

As compared to related work [3-6], our proposed MUCPW emphasizes on developing algorithms for multi-UAV collaborative area partition and coverage planning, taking into account the impact of wind speeds and directions on UAV battery consumption, which is indicated in Table 1.

TABLE I. COMPARISON OF RELATED RESEARCHES

Research	Multi-UAV collaborative area partition	UAV coverage planning for the shortest search time	Impact of wind speeds and directions on UAV battery consumption
[3]	No	No	No
[4]	No	No	No
[5]	No	No	No
[6]	No	No	No
MUCPW	Yes	Yes	Yes

3.Impact of Wind fields on UAV Power Consumption

3.1 UAV Hovering and Horizontal Flight on Power Consumption

The work in [3] conducts comprehensive tests on UAV power consumption, specifically focusing on hovering, horizontal and vertical movements. The results indicate a proportional relationship between UAV hover height and power consumption. In Equation 1, UAV_{height}^{hover} denotes the power consumption of hovering at *height*, $UAV_{initial}^{hover}$ denotes the power consumption at the lowest hovering height, i.e., 2.5 meters, $H_{hover}^{weights}(\%)$ is the extra percentage of power consumption for hovering at *height* over that at the lowest hovering height, the current height of the UAV is denoted as $UAV_{current}^{height(cm)}$, and the lowest hovering height is $UAV_{initial}^{height(cm)}$.

$$UAV_{height}^{hover} = UAV_{initial}^{hover} \times H_{hover}^{weights}(\%),$$

$$H_{hover}^{weights}(\%) = 1.03035^{\frac{UAV_{current}^{height(cm)} - UAV_{initial}^{height(cm)}}{50(cm)}} \quad (1)$$

Equation 2 represents $UAV_{height}^{fly}(W)$, which is the power consumption of UAV horizontal flight at height of 3 meters without considering wind fields. For UAV horizontal flight at a height of 3 meters, the additional percentage of power consumption, i.e., $H_{fly}^{weights}$, compared to hovering is 1.035%.

$$UAV_{height}^{fly}(W) = UAV_{height}^{hover} \times H_{fly}^{weights}(\%)$$

$$H_{fly}^{weights}(\%) = 1.035\% \quad (2)$$

Additionally, it is crucial to consider the impact of wind fields during UAV flight. In the work [4], tests were conducted on UAVs at a height of 1 meter above ground for wind speeds ranging from 4 to 12 meters per second. The results indicate that the actual power consumption of UAVs increases slowly for wind speeds of 1 to 4 meters per second, a gradual increase on power consumption from 4 to 7 meters per second, but a noticeable upward trend in power consumption for wind speeds ranging from 7 to 12 meters per second, which is formulated by Equation 3. The power consumption (W) of UAV horizontal flight at *height* with *windspeed* is defined as $UAV_{height}^{fly-wind}(W)$.

$$UAV_{height}^{fly-wind}(W) = 1.78606^{windspeed(m/s)} + UAV_{height}^{fly}(W) \quad (3)$$

3.2 The Impact of Wind Speed and Direction on UAV Power Consumption

During the mission, when the UAV traverses back and forth in a region, it may encounter different wind fields, resulting in varying impacts on UAV power consumption. In [2], the impact of wind on UAV's yaw angle is discussed. Assuming the UAV intends to fly from point A to point B along the planned green path shown in Fig. 1, with the wind blowing from the north to the left side of the UAV, the wind will deviate the UAV from the intended path. If the UAV does not make any direction correction, it will eventually follow the actual red path and reach point B'.

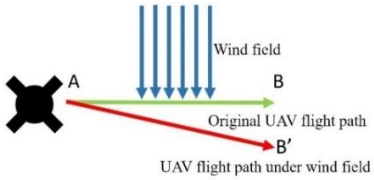

Fig.1. Relationship between wind and UAV flight path

Fig. 2 illustrates an example of the impact of the wind field on UAV. The green line segments represent UAV flight, including the heading angle UAV_{cource} measured in degrees from 0° and the airspeed $UAV_{airspeed}$. The blue line segments represent the wind field, including the wind direction $\text{W}_{\text{direction}}$ and windspeed W_{speed}. The corrected angle and flight speed for the UAV after experiencing the wind are denoted as $UAV_{\text{CorrectedAngle}}$ and $UAV_{\text{CorrectedAngle}}^{speed}$, respectively. The relationship among them is as follows. The vector formed by the UAV flight to the destination is equal to the vector of the UAV flight after wind correction plus the vector of the wind field. In Fig. 2, the wind field is represented by the blue triangular region. The vertical and horizontal projections of the wind field are given by $W_{speed} \times \sin(W_{direction})$ and $W_{speed} \times \cos(W_{direction})$, respectively. The vertical and horizontal projections of the UAV flight vector after wind correction are $UAV_{\text{CorrectedAngle}}^{speed} \times \sin(UAV_{\text{CorrectedAngle}})$ and $UAV_{\text{CorrectedAngle}}^{speed} \times \cos(UAV_{\text{CorrectedAngle}})$, respectively. Hence, subtracting the vertical projection of the wind field vector from the vertical projection of the vector of UAV flight to the destination yields the vertical projection of the UAV flight vector after wind correction, which is denoted as $Vertical\_Speed$ and formulated by Equation 4. Similarly, subtracting the horizontal projection of the wind field vector from the horizontal projection of the vector of UAV flight to the

destination yields the horizontal projection of the UAV flight vector after wind correction, which is is denoted as $Horizontal\_Speed$ and formulated by Equation 5. Finally, the corrected angle and speed of the UAV under the wind field are denoted as $UAV_{\text{CorrectedAngle}}$ and $UAV^{speed}_{\text{CorrectedAngle}}$, which are formulated by Equations 6 and 7 respectively.

$$Vertical\_Speed = UAV^{speed}_{\text{CorrectedAngle}} \times \sin\left(UAV_{\text{CorrectedAngle}}\right) = UAV_{airspeed} \times \sin(UAV_{cource}) - W_{speed} \times \sin(W_{direction}) \quad (4)$$

$$Horizontal\_Speed = UAV^{speed}_{\text{CorrectedAngle}} \times \cos\left(UAV_{\text{CorrectedAngle}}\right) = UAV_{airspeed} \times \cos(UAV_{cource}) - W_{speed} \times \cos(W_{direction}) \quad (5)$$

$$UAV_{\text{CorrectedAngle}} = tan^{-1}\frac{Vertical\_Speed}{Horizontal\_Speed} \quad (6)$$

$$UAV^{speed}_{\text{CorrectedAngle}} = \sqrt{Vertical\_Speed^2 + Horizontal\_Speed^2} \quad (7)$$

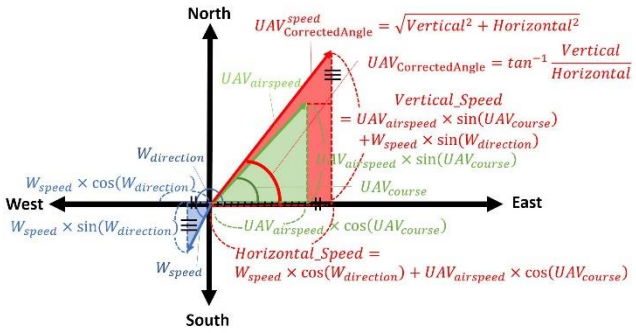

Fig.2. The corrected angle and speed of the UAV under the wind field

The following calculates the horizontal hover power consumption $UAV^{hover-wind}_{height}(W)$ and flight power consumption $UAV^{fly-wind}_{height}(W)$ of the UAV under the wind field. When the wind speed is W_{speed}, for the UAV to hover at a fixed position, it must resist the wind by flying at a speed W_{speed} opposite to the wind direction to stay stationary. Therefore, the horizontal hover power consumption per unit of time $UAV^{hover-wind}_{height}(W)$ for the UAV at a height of 3 meters is the flight power consumption obtained by substituting the windspeed W_{speed} into Equation 3, which is formulated by Equation 8. $UAV^{fly-wind}_{height}(W)$ in Equation 9 represents the flight power consumption per unit time. It is calculated by substituting the corrected flight speed $UAV^{speed}_{\text{CorrectedAngle}}$ of the UAV obtained from Equation 7 into Equation 3.

$$UAV^{hover-wind}_{height}(W) = 1.78606^{W_{speed}(m/s)} + UAV^{fly}_{height}(W) \quad (8)$$

$$UAV^{fly-wind}_{height}(W) = 1.78606^{UAV^{speed}_{\text{CorrectedAngle}}(m/s)} + UAV^{fly}_{height}(W) \quad (9)$$

3.3 Power Consumption for Taking Photos

When each UAV individually searches a region, taking photos at each unit to confirm the presence of survivors is required [7]. Assuming S_T is the shooting time for taking photos in each unit, the UAV only needs to hover horizontally at the same height and resist the wind for S_T seconds before moving on to the next unit, until reaching the endpoint. Therefore, the energy consumption required for taking photos at *height* for S_T seconds is denoted as $E^{ST}_{height}(Wh)$, which is formulated by Equation 10, where $UAV^{hover-wind}_{height}(W)$ is the hover power consumption per unit time calculated by Equation 8.

$$E^{ST}_{height} = UAV^{hover-wind}_{height}(W) \times S_T \quad (10)$$

3.4 Total Mission Time and Total Power Consumption for the Search and Rescue Mission.

Assuming the UAV speed is $UAV_{airspeed}$, wind speed is W_{speed}, and wind direction is $W_{direction}$. When disaster occurs, the GCS dispatches multiple UAVs to execute the SAR mission. During the mission, each UAV undergoes three stages of power consumption, namely:

1) *UAV flight from GCS to the starting unit of the region:* Assuming GCS coordinates are (0,0) and the starting unit of the region is given by (x_s,y_s), the forward flight distance from GCS to the starting unit of the region D^{fly}_{for} is $\sqrt{x_s^2 + y_s^2}$. As fomulated by Equations 6 and 7, the corrected angle and corrected flight speed for the UAV under the wind field are $UAV^{for}_{CorrectedAngle}$ and $UAV^{for-speed}_{CorrectedAngle}$, respectively. Therefore, the time to fly from GCS to the starting unit is denoted as T^{fly}_{for} and equal to $\frac{D^{fly}_{for}}{UAV^{for-speed}_{CorrectedAngle}}$. Substituting this into Equation 9 yields the forward flight energy consumption $E^{for-fly-wind}_{height}(Wh)$ under the wind field, which is formaulted by Equation 11.

$$E^{for-fly-wind}_{height} = UAV^{for-fly-wind}_{height}(W) \times T^{fly}_{for} = \left(1.78606^{UAV^{for-speed}_{\text{CorrectedAngle}}\left(\frac{m}{s}\right)} + UAV^{fly}_{height}(W)\right) \times \frac{D^{fly}_{for}}{UAV^{for-speed}_{\text{CorrectedAngle}}} \quad (11)$$

2) *From the starting unit of the region, the UAV follows the planned flight path, visits each unit and stays for S_T seconds to take photos until reaching the end unit of the region:* Assuming the UAV needs to visit a total of N units in the assigned region, where the UAV follows one of two major flying directions for N_1 units, resulting in a total of $(N_1 - 1)$ unit lengths. Similarly, the UAV follows another flying direction for N_2 units, resulting in $(N_2 - 1)$ unit lengths. Further, there are two kinds of turns to connect these two major flying directions mentioned above: one connects N_3 units, resulting in $(N_3 - 1)$ unit lengths and the other kind connects N_4 units, resulting in $(N_4 - 1)$ unit lengths. Their relationship is $N = N_1 + N_2 + N_3 + N_4 + 1$. In Fig. 3, there are N=32 units in a region under the 8×1 combination. After the UAV reaches to the starting unit at the upper left corner, it will follow a left-to-right flight direction to visit all units of the upper row with N_1=16 units and a total UAV flight distance of 15 units. On the other hand, it will follow a right-to-left flight direction to visit all units of the lower row until reaching the ending unit, which covers N_2=16 units and a total UAV flight distance of 15 units. There are two kinds of UAV flight turns to connect the upper and lower rows of units. Only the kind of turn which connects units from the

Ing-Chau Chang, Men-Yi Li,
Yu-Hsuan Hsieh, Chin-En Yen

upper row to the lower row exists in Fig. 3, resulting in a total UAV flight distance of 1 unit. Hence, different area divisions result in different values of these N_1, N_2, N_3 and N_4 values.

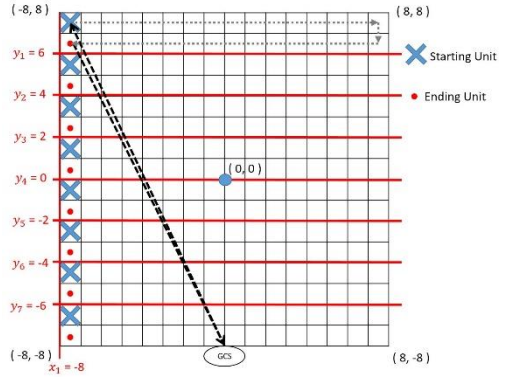

Fig.3. The UAV flight path for visiting all units of a region in the 8 × 1 area partition

Since the distance between any two units is the unit side length r, the flying time $T_{i,j}^{fly}$ between two consecutively visited units, denoted as i and j, is $\frac{r}{UAV_{\text{CorrectedAngle}}^{i,j-speed}}$, where $UAV_{\text{CorrectedAngle}}^{i,j-speed}$ is the corrected flight speed calculated by Equation 7. Then we can substitute the value into Equation 9 to obtain the flight power consumption between two units under the wind field, denoted as $E_{height}^{i,j-fly-wind}$, using Equation 12. Therefore, the total power consumption for visiting all units of the region, denoted as $E_{height}^{visit-fly-wind}$, can be calculated using Equation 13, and the total flying time is $T_{i,j}^{fly} \times N$. Because the power consumption required for taking photos for each unit at *height* is E_{height}^{ST}, the total power consumption for shooting photos for N units of a region is $E_{height}^{ST} \times N$ Therefore, the total power consumption $E_{height}^{visit-fly-ST-wind}$ for flying and taking photos against the wind field for all N units is given by Equation 14, and the total time for taking photos for all N units is $S_T \times N$.

$$E_{height}^{i,j-fly-wind} = UAV_{height}^{i,j-fly-wind}(W) \times T_{i,j}^{fly} = \left(1.78606^{UAV_{\text{CorrectedAngle}}^{i,j-speed}\left(\frac{m}{s}\right)} + UAV_{height}^{fly}(W)\right) \times \frac{r}{UAV_{\text{CorrectedAngle}}^{i,j-speed}} \quad (12)$$

$$E_{height}^{visit-fly-wind} = \sum_{i,j} E_{height}^{i,j-fly-wind} = \sum_{i,j}\left(1.78606^{UAV_{\text{CorrectedAngle}}^{i,j-speed}\left(\frac{m}{s}\right)} + UAV_{height}^{fly}(W)\right) \times \frac{r}{UAV_{\text{CorrectedAngle}}^{i,j-speed}} \quad (13)$$

$$E_{height}^{visit-fly-ST-wind} = E_{height}^{visit-fly-wind} + E_{height}^{ST} \times N = \sum_{i,j} E_{height}^{i,j-fly-wind} + E_{height}^{ST} \times N \quad (14)$$

3) UAV flight from the ending unit of the region back to GCS: Assuming GCS coordinates are (0, 0), and the ending unit of the region is given by (x_e, y_e), the backward distance D_{back}^{fly} between the ending unit and the GCS is $\sqrt{x_e^2 + y_e^2}$. Therefore, the time to fly from the ending unit back to the GCS under the wind field, denoted as T_{back}^{fly}, is $\frac{D_{back}^{fly}}{UAV_{CorrectedAngle}^{back-speed}}$. Substituting this into Equation 9 yields the flight power consumption $E_{height}^{back-fly-wind}$ for this backward stage by Equation 15.

$$E_{height}^{back-fly-wind} = UAV_{height}^{back-fly-wind}(W) \times T_{back}^{fly} = \left(1.78606^{UAV_{\text{CorrectedAngle}}^{back-speed}\left(\frac{m}{s}\right)} + UAV_{height}^{fly}(W)\right) \times \frac{D_{back}^{fly}}{UAV_{\text{CorrectedAngle}}^{back-speed}} \quad (15)$$

In summary, the total energy consumption $E^{SAR}(Wh)$ for visiting the region is the sum of Equations 11, 14, and 15, which is expressed by Equation 16. Finally, the total time for visiting the region is the sum of times spent in all three stages. After each UAV completes the search for all units of the assigned region, it will issue a message to the GCS to report whether the search target is found. Hence, the search time of the SAR mission is the sum of times spent in the first and second stages, which is formulated by Equation 17.

$$E^{SAR} = E_{height}^{for-fly-wind} + E_{height}^{visit-fly-ST-wind} + E_{height}^{back-fly-wind} = UAV_{\text{CorrectedAngle}}^{for-speed}(W) \times \frac{D_{for}^{fly}}{UAV_{\text{CorrectedAngle}}^{for-speed}} + \sum_{i,j} E_{height}^{i,j-fly-wind} + E_{height}^{ST} \times N + UAV_{height}^{back-fly-wind}(W) \times \frac{D_{back}^{fly}}{UAV_{\text{CorrectedAngle}}^{back-speed}} \quad (16)$$

$$T^{SAR} = T_{for}^{fly} + T_{i,j}^{fly} \times N = \frac{D_{for}^{fly}}{UAV_{\text{CorrectedAngle}}^{for-speed}} + \frac{r}{UAV_{\text{CorrectedAngle}}^{i,j-speed}} \times N \quad (17)$$

4.Time and Energy-Efficient Multi-UAV Coverage Planning

4.1 Area Partitioning Algorithm

Steps of the area partitioning algorithm in MUCPW are listed as follows. Assume the coordinates of the search area center is (0, 0) and the ending unit of each region is located at the unit closest to the GCS in the region.

a) First, find the factors of the number of dispatched UAVs. Assuming the number of UAVs is 8, its factors are 1, 2, 4, 8. Therefore, there are 4 possible factors. Save these factors into array UAV_{factor}^{array}. Then, find the factor combinations, which contains two factors and their product equal to the number of dispatched UAVs. Factor combinations of 8 are 8 × 1, 4 × 2, 2 × 4, and 1 × 8. Save these combinations into $UAV_{combination}^{array}$.

b) First, take two values of one factor combination from $UAV_{combination}^{array}$ as x_D and y_D. Second, divide the area along the x-axis and y-axis using Equations 18 and 19, where x_i is the i-th division on the x-axis, y_i is the i-th division on the y-axis, x_D is the number of total divisions on the x-axis, y_D is the number of total divisions on the y-axis, and n is half of the area side size. Fig. 3 shows area partition results of the 8 × 1 combination, where x_D, y_D and n are 1, 8, 8, respectively. Please note that the 8 × 1 combination divides the area into eight rows and one column here.

$$x_i = -n + \frac{2n}{x_D} \times (x_D - i) \quad (18)$$

$$y_i = -n + \frac{2n}{y_D} \times (y_D - i) \qquad (19)$$

c) Since the SAR mission requires every dispatched UAV reporting to the GCS whether the search target is found after each UAV completing the search for all units of the assigned region, the goal of the SAR mission is to minimize the search time for the most time-consuming region among all combinations. Equation 20 calculates the search time of the SAR mission for dispatching $x \times y$ UAVs, where the T_i^{SAR} is the search time of region *i*, calculated by Equation 17, of the $x \times y$ combination. Hence, the search time of eight UAVs is $Min(Max_i^{1\times8}(T_i^{SAR})$, $Max_i^{4\times2}(T_i^{SAR})$, $Max_i^{2\times4}(T_i^{SAR})$, $Max_i^{8\times1}(T_i^{SAR}))$.

$$ST^{SAR} = Min_{x,y}\left(Max_i^{x\times y}(T_i^{SAR})\right)$$

$$Max_i^{x\times y}(E_i^{SAR}) \le C \qquad (20)$$

Further, it is necessary to ensure that each UAV has sufficient battery power to return to the GCS after completing the SAR mission. Therefore, the total energy consumption, i.e., E_i^{SAR} calculated by Equation 16, on all three stages of the most time-consuming region for a feasible combination must be less than or equal to the UAV battery capacity *C*. Consequently, MUCPW finds a combination with the minimum search time among all combinations as the search time, i.e., ST^{SAR}, of the SAR mission, under the constraint that total energy consumption of this combination, i.e., $Max_i^{x\times y}(E_i^{SAR})$, is less than or equal to the UAV battery capacity, which is formulated by Equation 20.

4.2 MUCPW Searching Process

The search process of MUCPW is outlined as follows.

a) When an incident occurs and before the rescue team arrives, the GCS receives and designates the coordinates of the distressed individuals as the disaster center, which is denoted as the coordinate (0,0). The search area is then expanded along the x-axis and y-axis by n kilometers, forming a search area of $4n^2$ square kilometers. Hence, the coordinates of the four corners, i.e., top-left, top-right, bottom-left and bottom-right, of the area are (-n, n), (n, n), (-n, -n) and (n, -n), respectively.

b) Assuming that the GCS has *k* UAVs available, the search area is divided into $k \times x\%$ regions, with each region assigned one UAV for the search operation, while the remaining $k \times (1 - x\%)$ UAVs serve as backups. Once the number of dispatched UAVs is determined, the search area is segmented into regions equal to the number of dispatched UAVs. As mentioned above, the mission time and required energy consumption are calculated for each possible area partition combination. Equation 20 determines the optimal area partition combination with the corresponding mission search time ST^{SAR} and the mission energy consumption.

c) After determining the optimal area partition combination, GCS dispatches one UAV to visit each region by flying to the starting unit to commerse the search mission, as illustrated in Fig. 4 when n is 8, k is 10 and x is 80.

d) During the designated UAV search path, if survivors are detected, the UAV records the coordinates of them and issues messages to GCS, until the all units of the assigned region has been visited. After that, the UAV returns to GCS through the shortest fight path between the end unit of the region and GCS.

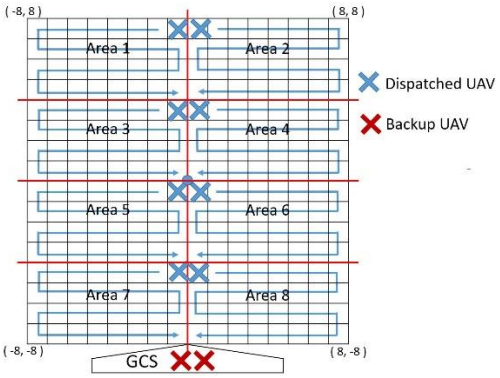

Fig.4. MUCPW determines the optimal area partition combination and dispatches one UAV to search each region

4.3 MUCPW-A Searching Process

From the MUCPW area partition result, it is observed that the UAV dispatched to the farther region from the GCS requires more search time and energy consumption as compared to those to nearer regions. Therefore, the adjustment of MUCPW, called MUCPW-A, aims to assign the dispatched UAVs with different region sizes according to the distance between the GCS and the region. As shown in Equation 21, the *i-th* division y_i on the y-axis of MUCPW-A is shifted 1 unit away the GCS as compared to that of MUCPW, while the divisions on the x-axis remains unchanged. If MUCPW-A results in a shorter mission time compared to MUCPW, the area partition combination of MUCPW-A is adopted.

$$y_i = -n + \frac{2n}{y_D} \times \left(y_D - i\right) + 1 \qquad (21)$$

5.Experiment and Results

The experimental simulation compares MUCPW and MUCPW-A with LSAR and LIAM. In the LIAM algorithm, UAVs perform random searches during the search phase, therefore, this simulation is conducted for ten thousand iterations to take the average values of two performance metrics. One is the mission time in minutes and the other is the corresponding energy consumption in Wh required for UAVs to complete the SAR process. They are shown as vertical axes of the simulation results. Two parameters are used as horizontal axes, one is the value of *n* of the area size, i.e., $(2n)^2$, ranging from 2 to 10 with the UAV number fixed at 8, and the other is the UAV number ranging from 2 to 10 with the value of *n* of the area size fixed at 8. The camera FOV is set at 179.3124589 degrees, UAV flight height is 3 meters, the unit side length is 1 km, UAV flying speed is $10\mathrm{m/s}$, wind speed is $5\mathrm{m/s}$ and wind direction is 180 degrees.

Fig. 5 illustrates simulation results conducted on five *n* values of area sizes $(2n)^2$. In general, a shorter UAV flight path for the entire mission under the given wind field implies a faster completion of the mission. The mission time of all searching algorithms grow as the value of *n*. Because LSAR focusing more on the disaster center, it assigns more numbers of UAVs and higher weights to regions closer to the center, which leads to a longer overall mission time under the wind field as compared to the proposed MUCPW and MUCPW-A. Without the prior knowledge of survivors' locations, LIAM explores the search area randomly during the searching phase. Due to the random search approach, LIAM exhibits the longest mission time among all. Results in Fig. 5 show that MUCPW and MUCPW-A spend significantly less mission

time compared to LIAM and LSAR under the wind conditions.

Fig. 6 illustrates the corresponding energy consumptions for these searching methods. When values of *n* are 2 and 4, LIAM consumes the least energy, followed by MUCPW and MUCPW-A, but LSAR exhibits the highest energy consumption. As the value of *n* continues to increase, energy consumption of LIAM significantly rises, with a growth rate much higher than the other three methods but LSAR, MUCPW and MUCPW-A consume similar energy. The SAR process focuses on minimizing the mission time, or in other words, minimizing the time needed to complete the last unit in a region. This implies that how to partition the search area into regions with different numbers of units to achieve the minimum mission time and corresponding energy consumption is crucial. Moreover, the efficient searching method should achieve fair energy consumption (Wh) to avoid asymmetric component losses and degradation of battery performance among all dispatched UAVs. In Fig. 7, it is evident that standard deviations of the energy consumption (Wh) of MUCPW and MUCPW-A are lower than the other two methods. This indicates that MUCPW and MUCPW-A ensure more equitable energy consumption among UAVs dispatched to various regions. When the value of *n* is 4, MUCPW-A has a standard deviation of the energy consumption 75.23, lower than 83.41 of MUCPW, indicating that the area partition combination of MUCPW-A results in more evenly distributed energy consumption among all UAVs.

In Fig. 8, experiments were conducted with five different number of UAVs. MUCPW and MUCPW-A consistently outperform the other two methods in terms of the mission time. Although LIAM shows a noticeable decrease when the number of UAV increases from 2 to 4, it remains higher than the other three methods when there are 8 to 10 UAVs. LSAR remains higher than MUCPW and MUCPW-A as it grows from 2 to 10 UAVs. Fig. 9 illustrates the required energy consumption, where MUCPW and MUCPW-A are notably superior to LIAM with two UAVs, similar to LSAR. As the the number of UAV increases, the differences among them diminish. MUCPW and MUCPW-A exhibit significantly lower standard deviations of energy consumption, as shown in Fig. 10, than LSAR and LIAM.

6. Conclusion

This paper proposes the MUCPW and MUCPW-A searching algorithms to assist search and rescue missions by dividing the search area into several regions based on the number of available UAVs in GCS when the mission commences. Considering environmental factors such as UAV flight height, wind direction and wind speed, the algorithm formulates equations to calculate the minimum mission time and corresponding energy consumption among all possible area partition methods, according to the horizontal or vertical search directions. MUCPW divides the area into equal sizes of regions, aiming for nearly equal mission paths for each UAV. MUCPW-A further adjusts region sizes according to the distance between the GCS and the region. Simulation results demonstrate that MUCPW and MUCPW-A require less mission time and no higher UAV energy consumption than those of the other two methods. Further, MUCPW-A exhibits the smallest standard deviation in energy consumption, signifying a more evenly distributed energy consumption among UAVs dispatched to various regions.

References

[1] S. Iranmanesh, R. Raad, M. S. Raheel, F. Tubbal and T. Jan, "Novel DTN Mobility-Driven Routing in Autonomous Drone Logistics Networks," IEEE Access, vol. 8, pp. 13661-13673, December 2019.

[2] M. Coombes, W. -H. Chen and C. Liu, "Boustrophedon coverage path planning for UAV aerial surveys in wind," 2017 International Conference on Unmanned Aircraft Systems (ICUAS), Miami, FL, USA, 2017, pp. 1563-1571

[3] X. Yu, S. Jin, D. Shi, L. Li, Y. Kang and J. Zou, "Balanced Multi-Region Coverage Path Planning for Unmanned Aerial Vehicles," 2020 IEEE International Conference on Systems, Man, and Cybernetics (SMC), Toronto, ON, Canada, 2020, pp. 3499-3506

[4] Y. Yaguchi and T. Tomeba, "Region Coverage Flight Path Planning Using Multiple UAVs to Monitor the Huge Areas," 2021 International Conference on Unmanned Aircraft Systems (ICUAS), Athens, Greece, 2021, pp. 1677-1682

[5] Heba A. Kurdi, Ebtesam Aloboud, Maram Alalwan, Sarah Alhassan, Ebtehal Alotaibi, Guillermo Bautista, Jonathan P. How, "Autonomous Task Allocation for Multi-UAV Systems Based on the Locust Elastic Behavior," Applied Soft Computing, Vol. 71, pp. 110-126, 2018.

[6] E. T. Alotaibi, S. S. Alqefari and A. Koubaa, "LSAR-Multi-UAV Collaboration for Search and Rescue Missions," IEEE Access, Vol. 7, pp. 55817-55832, 2019.

[7] Katharin R. Jensen-Nau, Tucher Hermans, kam K. Leang, "Reinforcement Learning-Based Collision Avoidance and Optimal Trajectory Planning in UAV Communication Networks," IEEE Transactions on Mobile Computing, Vol. 21, No. 1, pp. 306-320, 2022.

Contribution of Individual Authors to the Creation of a Scientific Article (Ghostwriting Policy)

The authors equally contributed in the present research, at all stages from the formulation of the problem to the final findings and solution.

Sources of Funding for Research Presented in a Scientific Article or Scientific Article Itself

No funding was received for conducting this study.

Conflict of Interest

The authors have no conflicts of interest to declare that are relevant to the content of this article.

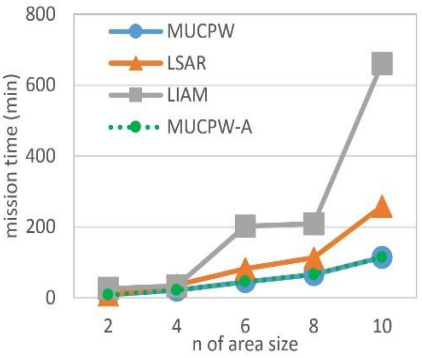

Fig.5. The value of n of the area size vs. the mission time

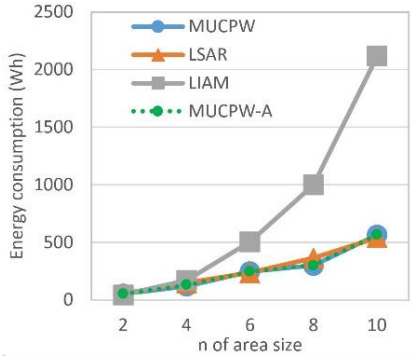

Fig.6. The value of n of the area size vs. energy consumption

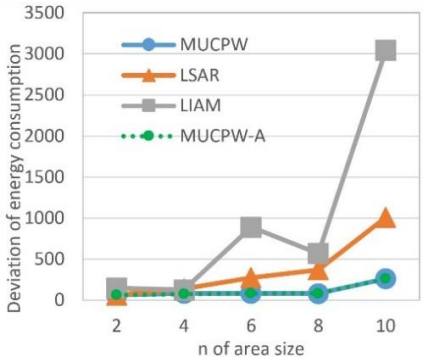

Fig.7. The value of n of the area size vs. the deviation of energy consumption

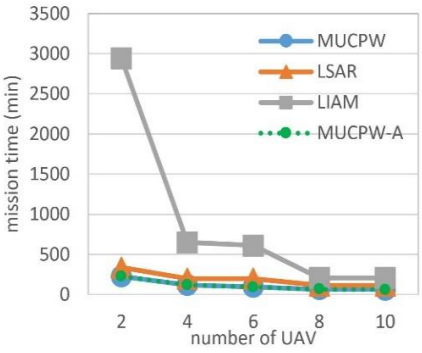

Fig.8. The number of UAV vs. the mission time

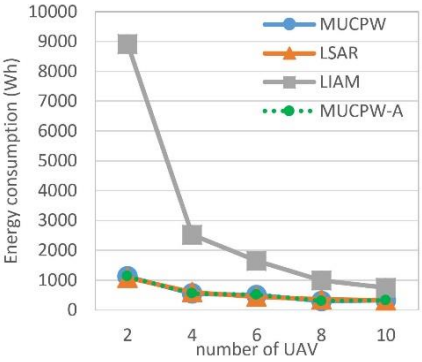

Fig.9. The number of UAV vs. energy consumption

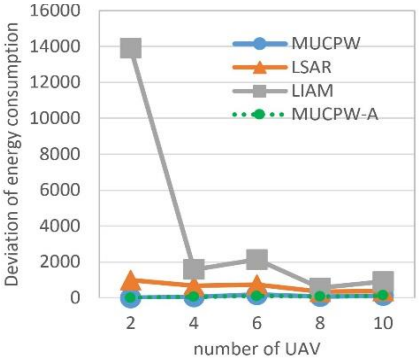

Fig.10. The number of UAV vs. the deviation of energy consumption